

# Electrochemical Stability of HAP-CNT/Ti6Al4V in Cell Culture Media

Diana K. Sierra-Herrera<sup>\*</sup>, Nerly D. Montañez, Sergio Blanco, Dario Y. Peña

Universidad Industrial de Santander, Bucaramanga, Colombia. Calle 9, Carrera 27, ciudad universitaria  
 diana.sierra4@correo.uis.edu.co

Ti6Al4V ELI alloys are widely used for orthopedic implants. These alloys have shown high corrosion resistance and biocompatibility. The limitation for their use are related to their poor bioactivity, hence the implants need a surface modification with materials that are able to promote bone tissue regeneration. With this objective, different surface modifications have been evaluated. Calcium phosphate coatings have shown high biocompatibility, bioactivity, and nontoxicity. The electrodeposition techniques show high efficiency, are easy to use, low cost and the coatings could be applied to irregular objects. In this work, we evaluated the electrochemical stability of Hydroxyapatite (HAP) with the incorporation of multiwall carbon nanotubes (MWCNT) on Ti6Al4V. We obtained HAP and HAP-MWCNT coatings on Ti6Al4V by pulsed electrodeposition. The obtained coatings were characterized by FTIR and XRD to evaluate the presence of MWCNT and calcium phosphates phases. The morphological and chemical composition evaluation was performed by SEM microscopy. The corrosion process was evaluated in cell culture media (RPMI-1640) by open circuit potential measurement, electrochemical spectroscopy impedance and linear sweep voltammetry to understand the kinetic of the dissolution. The results showed a relationship between the MWCNT incorporation, the resistivity of the coating and the stability of the passivation layer.

## 1. Introduction

The materials used in orthopedic implants, besides having mechanical properties according to their application have to exhibit good biocompatibility and bioactivity. Titanium alloys (Ti6Al4V) have been used for osteosynthesis due to their good biocompatibility and high corrosion resistance, further their Young's modulus are lower than other metals used in implants, having a closer value to the cortical bone Young's modulus (Chen and Thouas, 2015) (Elias et al., 2008). However, bone regeneration is not promoted by titanium alloys. In order to improve the interaction between titanium alloys and the human body, these alloys have been coated with materials that facilitate their osseointegration, among these are calcium phosphates, especially hydroxyapatite (HAP) (Asri et al., 2016). HAP is a bioceramic material present in the mineral phase of bones and can be synthesized by physical and chemical methods, and have good adaptation to in vivo conditions. Nevertheless, its brittle nature restricts its clinical application under load-bearing conditions (Hench and Jones, 2005). The incorporation of multiwall carbon nanotubes (MWCNT) as a reinforcing material into HAP matrix can improve its mechanical properties without affecting the bioactivity of the ceramic (Khanal et al., 2016). Coatings of HAP and HAP/MWCNT can be obtained with several methods such plasma spraying (Balani et al., 2007), electrophoretic method (Kaya et al., 2008) (Drevet et al., 2016), sol-gel (Maho et al., 2013) and electrodeposition (Prodana et al., 2015). Specifically, pulsed electrodeposition has advantages such as low synthesis temperature, high control of the coating thickness and composition; also, it has a relatively low cost process. In this work, we produced HAP and HAP/MWCNT coatings on Ti6Al4V by pulse electrodeposition and we evaluated the electrochemical stability of its coatings in cell culture media RPMI 1640.

## 2. Experimental

### 2.1 Functionalization of MWCNT

The purification and modification of MWCNT were made with an average external tube diameter of 6-13 nm, applying three steps treatment. The first one was the immersion of the MWCNT in 9M HNO<sub>3</sub> heated at 110 °C for 3 h, after that, the MWCNT were immersed into NaOH at 25 °C for 1 h. Finally, MWCNT were immersed in 6M HCl at 110 °C for 6 h. Between each step the MWCNT were washed with deionized water and filtered. After the last step the MWCNT were dried at 80 °C for 12 h.

### 2.2 Electrodeposition of coatings

Commercially available Ti6Al4V bar 14 mm diameter were cut into discs of 3 mm thick and used as electrodes. The specimens were polished with sandpaper, cleaned with acetone and water, pre-etched in an acidic mixture (HNO<sub>3</sub>:HF:H<sub>2</sub>O = 3:1:10) for 30 s and rinsed with distilled water. Pulsed electrodeposition was carried out in a three-electrode cell with a standard silver-silver chloride (Ag/AgCl) reference electrode and a platinum mesh counter electrode, using a Gamry 600 potentiostat, applying pulses of potential  $E_{on} = -1.6$  V and  $E_{off} = 0$  V vs Ag/AgCl. Pulse on time ( $t_{on}$ ) was 30 s and off time ( $t_{off}$ ) 15 s and the total time of electrodeposition were 30 minutes. The electrolyte was composed of Calcium nitrate tetrahydrate (Ca(NO<sub>3</sub>)<sub>2</sub>·H<sub>2</sub>O) and Ammonium dihydrogen phosphate (NH<sub>4</sub>H<sub>2</sub>PO<sub>4</sub>), mixed with a Ca/P molar ratio of 1.67 and the MWCNT were added before stabilizing the pH value. The pH value was adjusted with ammonium hydroxide (NH<sub>4</sub>OH) to 6 and the temperature of the solution was maintained at 65 °C.

### 2.3 Physicochemical characterization

Morphological evaluation of the coatings were carried out by Quanta FEG-650 field emission scanning electron microscope (SEM); Bruker D8 advance X-ray diffractometer (XRD) with Cu K $\alpha$  radiation generated at 40kV and 40 mA was used for studying the crystallinity and the present phases on the coating. Fourier transform infrared spectroscopy (FT-IR) using Nicolet iS50 Spectrometer with ATR technique was used for analyzing the chemical composition of the coating, the spectrum range was from 2000 cm<sup>-1</sup> to 400 cm<sup>-1</sup> with a number of 64 scans at the resolution of 4 cm<sup>-1</sup>.

### 2.4 Electrochemical evaluation

For the electrochemical evaluation of Ti6Al4V, Ti6Al4V/HAP and Ti6Al4V/HAP-MWCNT electrodes, a conventional three-electrode cell was used, using a platinum wire as a counter electrode and saturated Calomel electrode as a reference. The electrochemical measurements such as open circuit potential (OCP), electrochemical impedance spectroscopic (EIS) and Linear sweep voltammetry (LSV) were carried out to evaluate the stability of the coating in cell culture media. The OCP was measured for 1 h, EIS was evaluated in a frequency range of 0.01 Hz to 10<sup>5</sup> Hz and LSV were measured in the potential range between -30 mV and +1200 mV vs open circuit potential at a scan rate of 0,166 mV/s.

## 3. Results and discussion

### 3.1 Physicochemical characterizations of the coating

Figure 1 shows SEM images of the HAP and HAP-MWCNT coatings; images (a) and (c) show a general view of the surfaces, both coatings present a homogeneous distribution on the surface with a complete coverage of the titanium alloy. The spherical pores observed in the coatings are related to the hydrogen evolution reaction, which occurs simultaneously with the HAP electrodeposition, the hydrogen bubbles are formed and detached progressively during the synthesis, without a relevant effect on the coating properties. The specific morphology of the HAP can be appreciated in images (b) and (d), exhibiting the typical needle-like structure of the HAP (Isa et al., 2012). Images (d) and (e) confirm the incorporation of MWCNT, they show the appearance of small noodles.

Figure 2A corresponds to the XRD patterns of the Ti6Al4V/HAP (blue line) and Ti6Al4V/HAP-MWCNT (red line) coatings. The results indicate that HAP crystals were successfully fabricated by pulsed electrodeposition. The main diffraction peaks are observed at 2 $\theta$  values for HA at 25.74°, 32.09°, 40.51° and 52.98°. These results are in agreement with International Center for Diffraction Data (ICDD). Figure 2B represents the FTIR spectra of the Ti6Al4V/HAP (blue line) and Ti6Al4V/HAP-MWCNT (red line) coatings. The characteristics absorption bands for HAP and Ca<sub>2</sub>P<sub>2</sub>O<sub>7</sub> have been reported in the literature (Berzina-Cimдина and Borodajenko, 2012) (Bih et al., 2006). The modes corresponding to PO<sub>4</sub><sup>3-</sup> groups appear at 471-600, 1024-1090 cm<sup>-1</sup> and for P<sub>2</sub>O<sub>7</sub> appear at 719, 923, 1165 and 1200 cm<sup>-1</sup> respectively. The trace at 471 cm<sup>-1</sup> is attributed to the band PO<sub>4</sub><sup>3-</sup> bending ( $\nu_2$ ), the bending mode for the phosphate group ( $\nu_4$ ) is reflected at 560 and 600 cm<sup>-1</sup>, the stretching mode is at 978 ( $\nu_1$ ) and stretching vibrations ( $\nu_3$ ) at 1024 and 1090 cm<sup>-1</sup>. The

bending vibrational modes of hydroxyl (OH<sup>-</sup>) group were identified at 624 cm<sup>-1</sup>. In fact, the FTIR spectra corroborate the results of XRD regarding the obtaintment of calcium phosphates coating by pulsed electrodeposition (He et al., 2016) (Gopi et al., 2012). However, no MWCNT peaks were found neither in the XRD patterns and nor in FTIR spectra indicating that the amount of MWCNT introduced into the coating is difficult to detect within the sensitivity limit of these techniques.

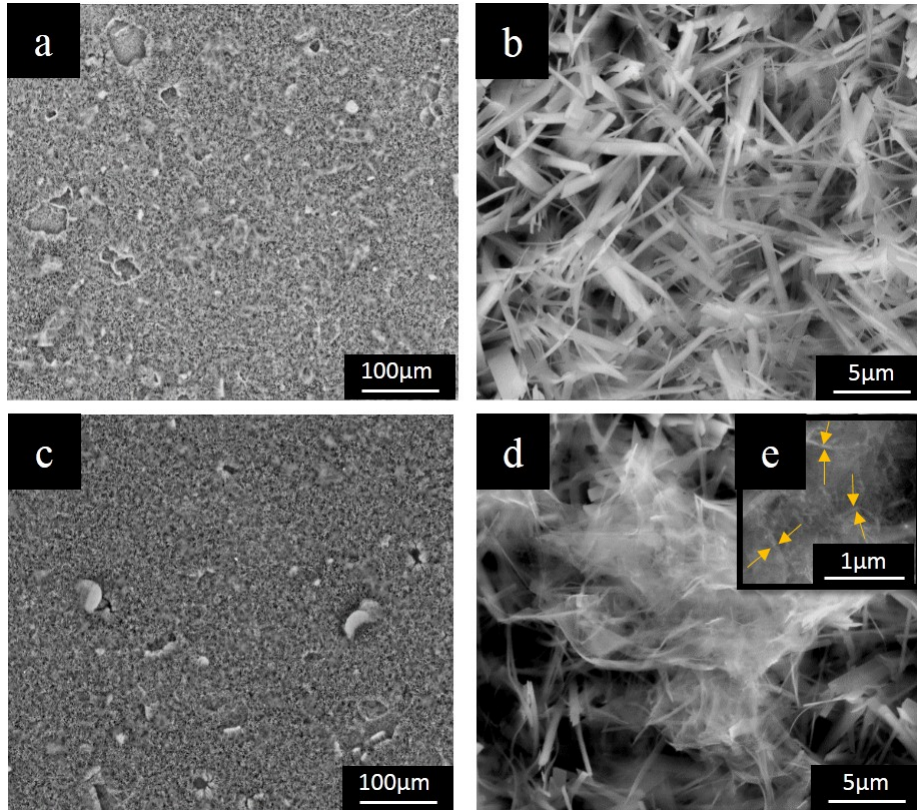


Figure 1: SEM images of coatings obtained by pulsed electrodeposition on Ti6Al4V (a-b) HAP (c-e) HAP-MWCNT.

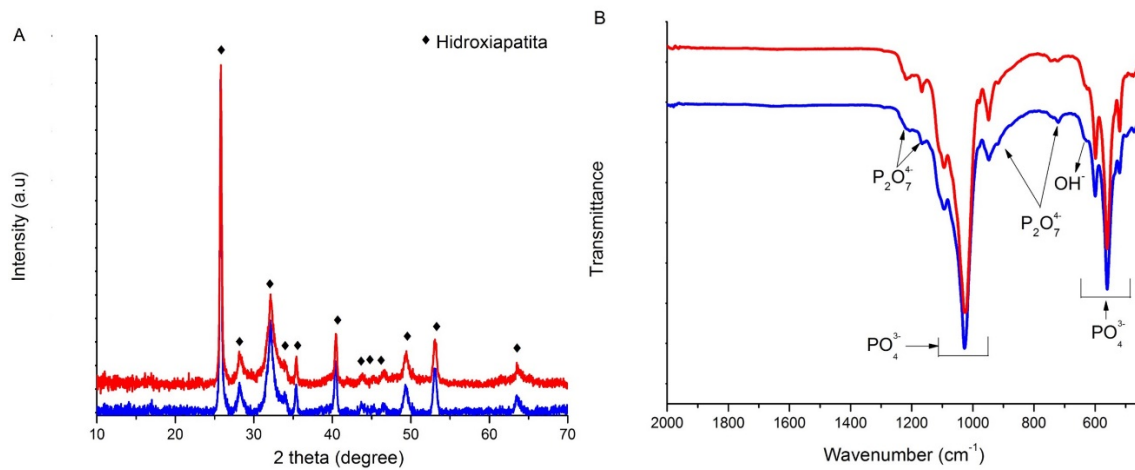


Figure 2: (A) XRD patterns of coating on Ti6Al4V (blue line) HAP (red line) HAP/CNT and (B) FTIR spectra of coating on Ti6Al4V (blue line) HAP (red line) HAP/CNT.

### 3.2 Electrochemical characterizations of the coating

Figure 3 shows the linear sweep voltammetry of Ti6Al4V, Ti6Al4V/HAP and Ti6Al4V/HAP-MWCNT electrodes evaluated in cell culture media RPMI 1640. Green line represent the electrochemical response of the Ti6Al4V electrode, this curve has the typical behavior of passive metals (Okazaki et al., 1998); where the dissolution of the electrode occurs under kinetic control since corrosion potential (-420 mV vs SCE) to -220 mV vs SCE, followed by the formation of the passive layer, where the current stays fixed ( $i_p = 1.54 \times 10^{-6} \text{ A.cm}^{-2}$ ). In the kinetic controlled zone, the current has an exponential dependence with the potential, represented by a line in Figure 3, this behavior is described by the Butler-Volmer equation (Bard et al., 1980), and the slope depends on some variables including the experimental temperature, Faraday and gas constants, exchange current density ( $i_0$ ) and the number of participating electrons. Comparing the experimental slope ( $\beta_a = 143 \text{ mV/dec}$ ) with the slopes obtained, varying the number of participating electrons, correspondence was obtained between experimental values and the theoretical model including one electron in the oxidation reaction (see insert). This value differs from the expected for the oxidation of the titanium, and it could be related to the alloying elements and the segregation of secondary phases, this hypothesis opens a new possibility in the corrosion mechanism study and will be studied in an upcoming work.

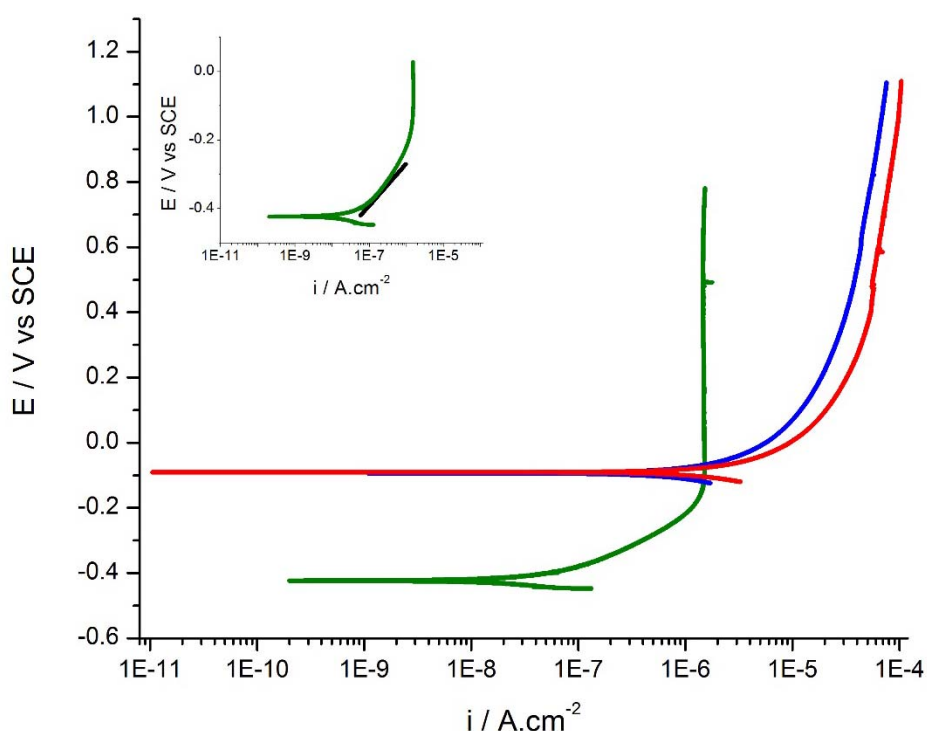


Figure 3: Linear sweep voltammetry curves in cell culture media RPMI 1640 for Ti6Al4V (green), Ti6Al4V/HAP (blue) and Ti6Al4V/HAP-CNT (red). Insert: comparison between Ti6Al4V and theoretical response for one transferred electron.

Blue line represents the response of the Ti6Al4V/HAP electrode. With the application of the coating, the corrosion potential shift to more positive values and the current response does not show the typical behavior of the passive layer. In this case the anodic currents could be divided into three zones: the first one, between the corrosion potential (-91 mV vs SCE) and 14 mV vs SCE, where the current shows a linear increment with the applied overpotential, with a Tafel slope of 153 mV/dec, similar to the value obtained for the Ti6Al4V electrode, related to the electrochemical oxidation of the Ti alloy under kinetic control; the second zone between 14 and 310 mV vs SCE, where the current shows an exponential increment which is a transition among the first and third zone, related to a mix control. The last zone, for potentials over 310 mV vs SCE, the current shows a linear increment in function of the applied potential, in this case the slope value (770 mV/dec) is higher than the maximum slope value that could be related to a kinetic control using the Butler-Volmer equation (Bard et al., 1980). Then, this behavior is the response of a mixed controlled dissolution and the passive layer; it is attributed to the HAP coating effect, where the coating is dissolved progressively which is favorable because promote bones ingrowth and adhesion on the surface on the implant (Asri et al., 2016). The

electrochemical response of HAP is according to the morphology observed in SEM images (Figure 1), where the open structure allows the interaction of ions between the titanium alloy and the surrounded electrolyte. The response of the Ti6Al4V/HAP-MWCNT (red line) has a similar behavior of the Ti6Al4V/HAP, with a small increment in the registered current values in each potential, which agrees with the expected behavior, because the MWCNT are inert in this electrolyte and do not modify the electrochemical reactions. The increment in the registered current in comparison with the Ti6Al4V/HAP electrode is related to the good electrical conductivity of the MWCNT. Table 1 summarizes the characteristic values of the electrodes.

Table 1: Characteristic values of the electrodes obtained from the linear sweep voltammetry analysis.

Electrode	$i_0 / \text{A.cm}^{-2}$	$E_{\text{corr}} / \text{mV vs SCE}$	$i_0 / \text{A.cm}^{-2}$	$\beta_a (\text{mV/dec})$
Ti6Al4V	$6,6 \times 10^{-8}$	-420	$1,54 \times 10^{-6}$	143
Ti6Al4V/HAP	$1,5 \times 10^{-6}$	-91	-	153
Ti6Al4V/HAP-MWCNT	$2,4 \times 10^{-6}$	-90	-	115

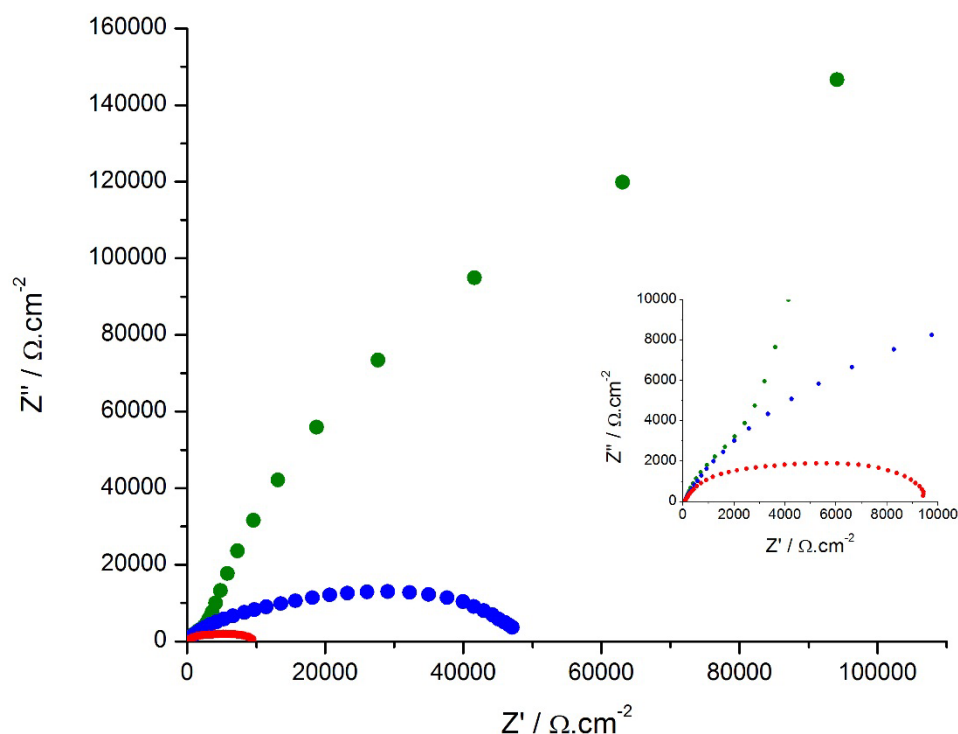


Figure 4: Nyquist plot in cell culture media RPMI 1640 for Ti6Al4V (green), Ti6Al4V/HAP (blue) and Ti6Al4V/HAP-CNT (red). Insert: detail of the small values resistance zone.

Results show in the Nyquist plot (Figure 4) are in agree with the linear sweep voltammetry. With the application of the HAP coating, the charge transfer resistance ( $R_{ct}$ ) shows an important reduction, this variation was expected if we compare the exchange current density values showed in table 1, because the  $R_{ct}$  is inversely proportional to  $i_0$ . Additionally, it is evident that the responses of the coated electrodes have two time constants generating a “flattened” semicircle composed by two overlapping semicircles; this variation is produced because the HAP has its own resistance to the transport of charges. It has shown the same effect with the Ti6Al4V/HAP-MWCNT electrode (insert in Figure 4) that have the lowest resistance due to the conductivity of the MWCNT.

#### 4. Conclusions

The results obtained by SEM, DRX, FTIR confirmed that: the composition of coatings are calcium phosphates (HAP), besides of corroborating that the use of pulsed electrodeposition we can obtain the incorporation of MWCNT into the HAP coating on Ti6Al4V. With the coating of HAP and HAP/MWCNT we could observe a significant variation in the electrochemical behavior, modifying the stability of the passive layer and therefore

enhances its biocompatibility. Moreover, we can evidence the effect in the resistivity of the coating by the incorporation of the MWCNT, which improves the dissolution of the coating, enhancing osseous tissue ingrowth.

### Acknowledgment

The authors want to thank Jaimes Rueda & Cia Ltda, Universidad Industrial de Santander, Vicerrectoria de Investigación y Extension and Grupo de Investigaciones en Corrosion for funding this Project under internal code 1888 and X-Ray Diffraction Laboratory Parque Tecnológico Guatiguara by diffraction analysis.

### Reference

- Asri R. I. M., Harun W. S. W., Hassan M. A., Ghani S. A. C., Buyong Z., 2016, A review of hydroxyapatite-based coating techniques: Sol-gel and electrochemical depositions on biocompatible metals, *Journal of the Mechanical Behavior of Biomedical Materials*, 57, 95-108. DOI: 10.1016/j.jmbbm.2015.11.031
- Balani K., Anderson R., Laha T., Andara M., Tercero J., Crumpler E., Agarwal A., 2007, Plasma-sprayed carbon nanotube reinforced hydroxyapatite coatings and their interaction with human osteoblasts in vitro, *Biomaterials*, 28, 618–624. DOI:10.1016/j.biomaterials.2006.09.013
- Bard A. J., Faulkner L. R., Leddy J., Zoski C. G., 1980, *Electrochemical methods: fundamentals and applications* (Vol. 2). New York: Wiley.
- Berzina-Cimdina L., Borodajenko N., 2012, Research of calcium phosphates using Fourier transform infrared spectroscopy. In *Infrared Spectroscopy-Materials Science, Engineering and Technology*. InTech, Rijeka, Croatia
- Bih H., Saadoune I., Mansori M., 2006, The lamellar  $\text{Na}_2\text{CoP}_2\text{O}_7$  pyrophosphate: Preparation, structural and spectroscopic studies, *Journal of Condensed Mater*, 7, 74-76.
- Chen Q., Thouas G. A., 2015. *Metallic implant biomaterials*. *Materials Science and Engineering R: Reports*, 87, 1-57, DOI:10.1016/j.mser.2014.10.001
- Drevet R., Ben Jaber N., Faur J., Tara A., Ben Cheikh Larbi A., Benhayoune H., 2016, Electrophoretic deposition (EPD) of nano-hydroxyapatite coatings with improved mechanical properties on prosthetic Ti6Al4V substrates, *Surface and Coatings Technology*, 301, 94-99, DOI: 10.1016/j.surfcoat.2015.12.058
- Elias C. N., Lima J. H. C., Valiev R., Meyers M. A., 2008, Biomedical applications of titanium and its alloys. *Jom*, 60(3), 46-49.
- Gopi D., Indira J., Kavitha L., 2012, A comparative study on the direct and pulsed current electrodeposition of hydroxyapatite coatings on surgical grade stainless steel, *Surface and Coatings Technology*, 206, 2859-2869, DOI: 10.1016/j.surfcoat.2011.12.011
- He D. H., Wang P., Liu P., Liu X. K., Ma F. C., Zhao J., 2016, HA coating fabricated by electrochemical deposition on modified Ti6Al4V alloy, *Surface and Coatings Technology*, 301, 6–12. DOI: 10.1016/j.surfcoat.2016.07.005
- Hench L. L., Jones J. R., *Institute of Materials, M.*, 2005, *Biomaterials, artificial organs and tissue engineering* (Woodhead P). CRC Press.
- Isa N. N. C., Mohd Y., Yury N., 2012, Electrochemical Deposition and Characterization of Hydroxyapatite (HAp) on Titanium Substrate, *APCBEE Procedia*, 3, 46-52, DOI:10.1016/j.apcbee.2012.06.044
- Kaya C., Singh I., Boccaccini A. R., 2008, Multi-walled Carbon Nanotube-Reinforced Hydroxyapatite Layers on Ti6Al4V Medical Implants by Electrophoretic Deposition (EPD), *Advanced Engineering Materials*, 10, 131–138, DOI:10.1002/adem.200700241
- Khanal S. P., Mahfuz H., Rondinone A. J., Leventouri T., 2016, Improvement of the fracture toughness of hydroxyapatite (HAp) by incorporation of carboxyl functionalized single walled carbon nanotubes (CfSWCNTs) and nylon, *Materials Science and Engineering: C*, 60, 204-210, DOI:10.1016/j.msec.2015.11.030
- Maho A., Detriche S., Delhalle J., Mekhalif Z., 2013, Sol – gel synthesis of tantalum oxide and phosphonic acid-modified carbon nanotubes composite coatings on titanium surfaces, *Materials Science & Engineering C*, 33(5), 2686-2697, DOI:10.1016/j.msec.2013.02.025
- Okazaki Y., Rao S., Ito Y., Tateishi T., 1998, Corrosion resistance, mechanical properties, corrosion fatigue strength and cytocompatibility of new Ti alloys without Al and V, *Biomaterials*, 19(13), 1197-1215, DOI: 10.1016/S0142-9612(97)00235-4
- Prodana M., Duta M., Ionita D., Bojin D., Stan, M. S., Dinischiotu, A., Demetrescu, I., 2015, A new complex ceramic coating with carbon nanotubes, hydroxyapatite and TiO<sub>2</sub> nanotubes on Ti surface for biomedical applications, *Ceramics International*, 41(5), 6318–6325, DOI:10.1016/j.ceramint.2015.01.060